

---

## Depth Distribution Of The Maxima Of Extensive Air Shower

---

J. H. Adams, Jr.<sup>1</sup>, G. D'Ali Staiti<sup>2</sup>, L. W. Howell<sup>1</sup> and S. Piraino<sup>3</sup> (the EUSO Collaboration)

(1) NASA Marshall Space Flight Center, Huntsville, Alabama 35812 USA

(2) DIFTER, Universita di Palermo, Italy

(3) IASF-CNR, Palermo, Italy

---

### Abstract

Observations of extensive air showers from space can be free from interference by low altitude clouds and aerosols if the showers develop at a sufficiently high altitude. In this paper we explore the altitude distribution of shower maxima to determine the fraction of all showers that will reach their maxima at sufficient altitudes to avoid interference from these lower atmosphere phenomena. Typically the aerosols are confined within a planetary boundary layer that extends only 2-3 km above the earth's surface. Cloud top altitudes extend above 15 km but most are below 4 km. The results reported here show that more than 75% of the showers that will be observed by EUSO have maxima above the planetary boundary layer. The results also show that more than 50% of the showers that occur on cloudy days have their maxima above the cloud tops.

### 1. Pathlength Distributions

The pathlength distribution of shower maxima has been measured in the High Resolution Fly's Eye experiment[1]. Using the data on showers with energies between  $1.3 \times 10^{18}$  and  $2.5 \times 10^{18}$  eV, we have fit the measured distribution between 550 and 1000 g/cm<sup>2</sup> with the double exponential function in Eq. 1 as:

$$f(x) = \begin{cases} Ae^{bx}, & 550 \leq x \leq 710 \\ Ce^{dx}, & 710 < x \leq 1000 \end{cases} \quad (1)$$

The coefficients were estimated to be  $A = 5.07917 \times 10^{-8}$ ,  $b = 0.0170627$ ,  $C = 5613.27$ , and  $d = -0.018752$ . This probability density function is depicted as the leftmost curve in Fig. 1. To obtain the distribution at the higher energies of interest (e.g.  $1 \times 10^{19}$ ,  $1 \times 10^{20}$ , and  $1 \times 10^{21}$  eV),  $f(x)$  was shifted by 50, 100, and 160 g/cm<sup>2</sup>, respectively, so that the mean of the shifted distributions would coincide with the mean elongation rates shown in Fig. 9 of [1]. The resulting distributions are also shown in Fig. 1.

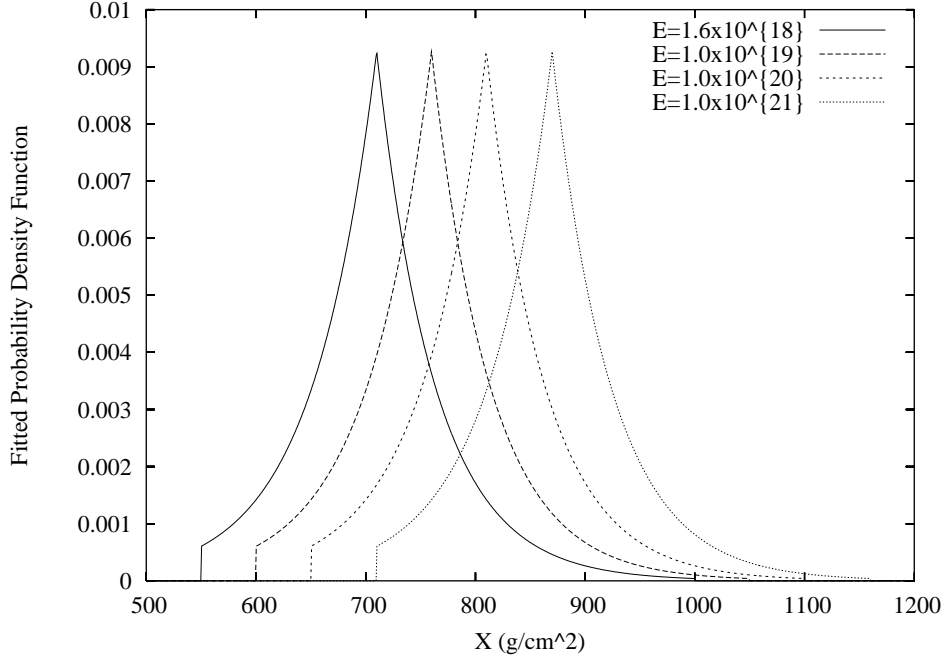


**Fig. 1.** Fitted pathlength distribution for  $1.6 \times 10^{18}$ ,  $1 \times 10^{19}$ ,  $1 \times 10^{20}$ , and  $1 \times 10^{21}$  eV.

## 2. Atmospheric Depth Distributions

Next, we obtain the atmospheric depth distribution by convolving these pathlength distributions with the arrival direction distribution of cosmic rays. The cosmic rays are assumed to arrive isotropically (i.e. there are equal numbers in equal solid angle elements) so the distribution goes as the solid angle subtended by a flat area as a function of the zenith angle, i.e.  $\Omega = \pi \sin^2(\theta)$  where  $\theta$  is the zenith angle (0 at normal incidence). Thus, the probability density function for the arrival direction distribution of cosmic rays is

$$\omega(\theta) = 2 \sin(\theta) \cos(\theta), 0 \leq \theta \leq \pi/2 \quad (2)$$

Consequently, a cosmic ray having pathlength  $X$  and arrival direction  $\theta$  will have atmospheric depth  $D = X \cos(\theta)$  for the maximum of the shower. For notational convenience we introduce the random variable  $Y = \cos(\theta)$  and note that  $Y$  has probability density function

$$g(y) = 2y, 0 \leq y \leq 1 \quad (3)$$

Thus, the depth of shower maxima is  $D = XY$  and its probability density function follows from the theory of the distribution of the product of two random variables, to give

$$h(d) = \int_0^1 f(d/y)g(y)|J|dy \quad (4)$$

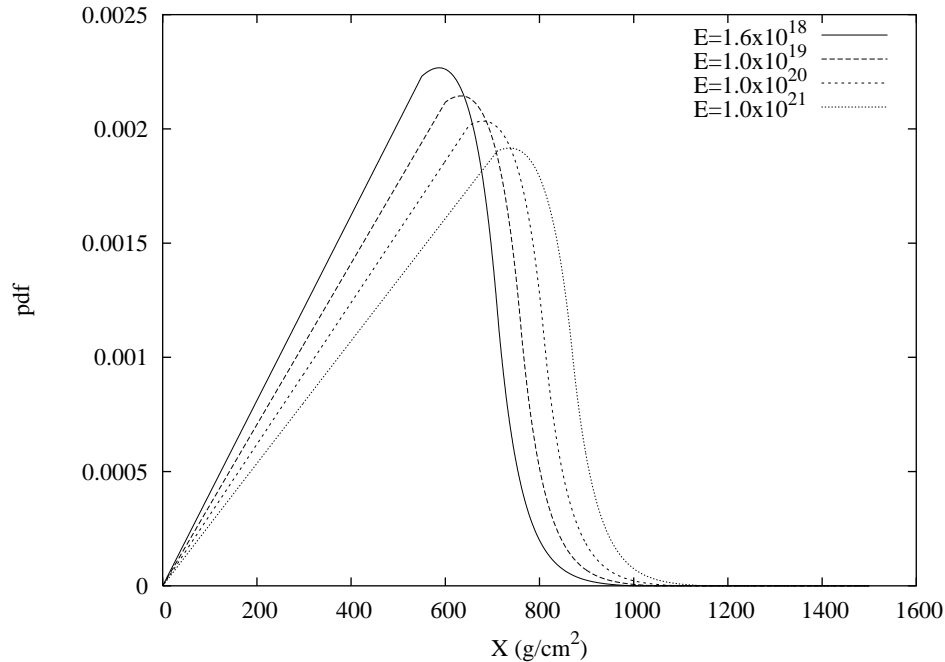


**Fig. 2.** The probability density function for the depths of shower maxima of extreme energy cosmic rays for four cosmic ray energies.

where  $|J| = 1/y$  is the Jacobian of the transformation.

We used eq. (4) with the four pathlength distributions of shower maxima at  $1.6 \times 10^{18}$ ,  $1.0 \times 10^{19}$ ,  $1.0 \times 10^{20}$ , and  $1.0 \times 10^{21}$  eV shown in Fig. 1. The resulting distributions are shown in Fig. 2 and corresponding integral distributions (cumulative distribution function) are shown in Fig. 3.

### 3. Results

We have used the data in Fig. 3 to determine the values of  $X$  such that 50%, 75%, 90%, 95%, and 99% of the showers have maxima at lesser depths,  $X$ . These are shown in Table 1. These depths are also converted into altitudes in km above sea level according to the 1976 US Standard Atmosphere[2].

### 4. References

1. Soloksky, P. 2002, "The High Resolution Flys Eye—Status and Preliminary Results on Cosmic Ray Composition Above  $10^{18}$  eV", private communication.
2. U. S. Standard Atmosphere 1976, U. S. Government Printing Office, Washington D. C., (<http://aero.stanford.edu/StdAtm.html>)

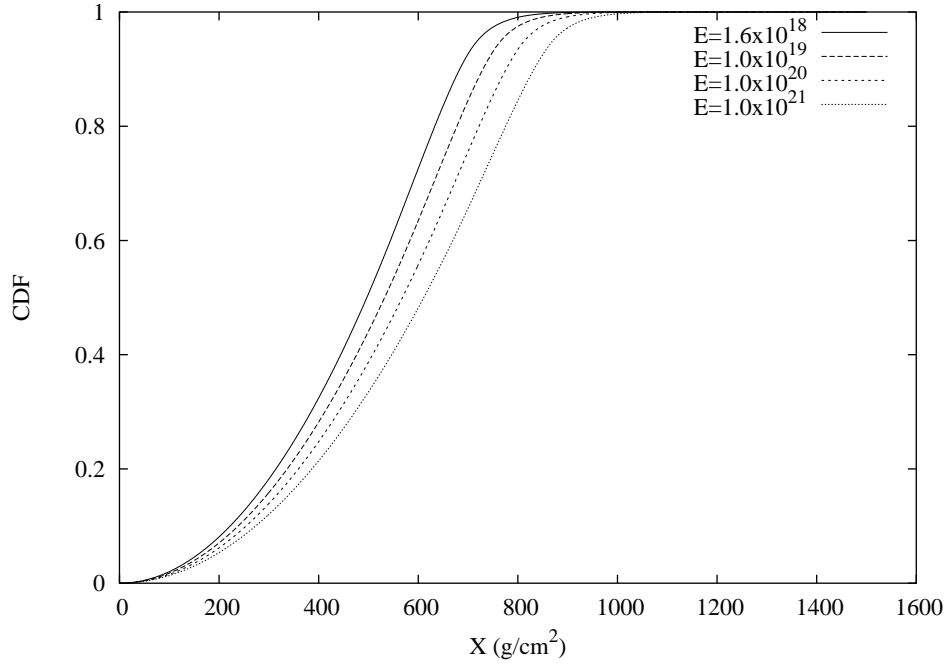


**Fig. 3.** The probability that shower maximum occurs at or above the atmospheric depth  $D$  in  $\text{g}/\text{cm}^2$  for four shower energies.

**Table 1.** This shows the depths in the atmosphere to which observations must extend to in order observe various fractions of all shower maxima at various energies. These depths are also converted into altitudes in km above sea level according to the 1976 US Standard Atmosphere[2].

P (%)	$1.6 \times 10^{18} \text{eV}$		$1 \times 10^{19} \text{eV}$		$1 \times 10^{20} \text{eV}$		$1 \times 10^{21} \text{eV}$	
	$\text{g}/\text{cm}^2$	km	$\text{g}/\text{cm}^2$	km	$\text{g}/\text{cm}^2$	km	$\text{g}/\text{cm}^2$	km
50	497	5.40	532	4.89	568	4.40	611	3.84
75	611	3.84	654	3.31	697	2.81	749	2.24
90	683	2.97	730	2.45	776	1.95	832	1.39
95	719	2.57	766	2.06	814	1.57	871	1.02
99	797	1.75	844	1.27	892	0.82	949	0.30